Physics – Uspekhi **61** (1) 99 – 104 (2018)

CONFERENCES AND SYMPOSIA

PACS numbers: **02.30. – f**, **02.50. – r**, **05.40. – a**

THE 100th ANNIVERSARY OF THE BIRTH OF I M LIFSHITZ

Rare-event statistics and modular invariance

S K Nechaev, K Polovnikov

DOI: https://doi.org/10.3367/UFNe.2017.01.038106

Contents

Abstract. Simple geometric arguments based on constructing the Euclid orchard are presented, which explain the equivalence of various types of distributions that result from rare-event statistics. In particular, the spectral density of the exponentially weighted ensemble of linear polymer chains is examined for its number-theoretic properties. It can be shown that the eigenvalue statistics of the corresponding adjacency matrices in the sparse regime show a peculiar hierarchical structure and are described by the popcorn (Thomae) function discontinuous in the dense set of rational numbers. Moreover, the spectral edge density distribution exhibits Lifshitz tails, reminiscent of 1D Anderson localization. Finally, a continuous approximation for the popcorn function is suggested based on the Dedekind η-function, and the hierarchical ultrametric structure of the popcorn-like distributions is demonstrated to be related to hidden $\mathrm{SL}(2, Z)$ modular symmetry.

Keywords: modular form, popcorn function, Dedekind function, spectrum of sparse matrix, Euclid's orchard, $\mathrm{SL}(2, Z)$ modular group, Lifshitz tails, Anderson localization

S K Nechaev Interdisciplinary Scientific Center Poncelet (ISCP), Bol'shoi Vlas'evskii per. 11, 119002 Moscow, Russian Federation; Lebedev Physical Institute, Russian Academy of Sciences, Leninskii prosp. 53, 119991 Moscow, Russian Federation
E-mail: sergei.nechaev@gmail.com
K Polovnikov Center for Energy Systems, Skolkovo Institute of Science and Technology, ul. Nobelya 3, 143005 Skolkovo, Moscow, Russian Federation; Lomonosov Moscow State University, Faculty of Physics, Leninskie gory 1, str. 2, 119992 Moscow, Russian Federation
E-mail: kipolovnikov@gmail.com

Received 24 February 2017
Uspekhi Fizicheskikh Nauk **188** (1) 106 – 112 (2018)
DOI: https://doi.org/10.3367/UFNr.2017.01.038106
Translated by S K Nechaev and K Polovnikov; edited by A Radzig

1. Introduction

The so-called 'popcorn function' [1], $g(x)$, also known as the Thomae function, also has many other names: the raindrop function, the countable cloud function, the modified Dirichlet function, the ruler function, etc. It is one of the simplest number-theoretic functions possessing a nontrivial fractal structure (another famous example is the everywhere continuous but never differentiable Weierstrass function). The popcorn function is defined in the open interval $x \in (0, 1)$ according to the following rule:

$$g(x) = \begin{cases} \dfrac{1}{q}\,, \text{ if } x = \dfrac{p}{q}\,, \ p \text{ and } q \text{ are coprime}\,, \\ 0\,, \text{ if } x \text{ is irrational}\,. \end{cases} \tag{1}$$

The popcorn function g is discontinuous at every rational point because irrationals come infinitely close to any rational number, while $g(x)$ vanishes at all irrationals. At the same time, g is continuous at irrationals.

One of the most beautiful incarnations of the popcorn function arises in a so-called 'Euclid orchard' representation. Consider an orchard of trees of *unit heights* located at every point (an, am) of a two-dimensional square lattice, where n and m are nonnegative integers defining the lattice, and a is the lattice spacing, $a = 1/\sqrt{2}$. Suppose we stay in the line $N = 1 - m$ between the points $\mathrm{A}(0, a)$ and $\mathrm{B}(a, 0)$, and observe the orchard grown in the first quadrant along the rays emitted from the origin $(0, 0)$ (Fig. 1).

Along these rays we see only the first open tree with coprime coordinates, $\mathrm{M}(ap, aq)$, while all other trees are shadowed. We introduce the auxiliary coordinate basis (x, y) with the x-axis along the segment AB and y normal to the orchard plane (as shown in Fig. 1a). We set the origin of the x-axis at the point A, then the point B has the coordinate $x = 1$. It is a nice school geometric problem to establish that: (i) having the focus located at the origin, the tree at the point $\mathrm{M}(ap, aq)$ is spotted at the place $x = p/(p + q)$, (ii) the *visible height* of this tree is $1/(p + q)$. In other words, the 'visibility

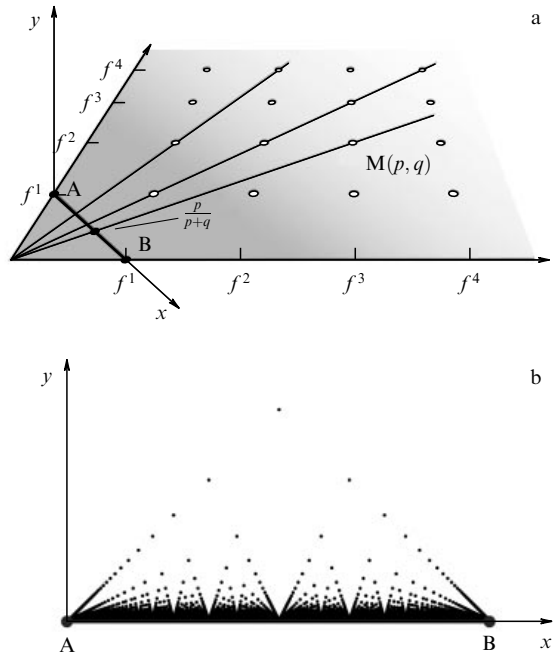

Figure 1. (a) Construction of the Euclid orchard; (b) popcorn (Thomae) function.

diagram' of such a lattice orchard is exactly the popcorn function.

The popcorn correspondence $p/q \to 1/q$ arises in the Euclid orchard problem as a purely geometrical result. However, the same function has appeared as a probability distribution in a plethora of biophysical and fundamental problems, such as the distribution of quotients of reads in DNA sequencing experiment [2], quantum $1/f$ noise and the Frenel–Landau shift [3], interactions of nonrelativistic ideal anions with a rational statistics parameter in the magnetic gauge approach [4], or the frequency of specific subgraphs counting in the protein–protein network of a *Drosophila* [5]. Though the extent of similarity with the original popcorn function could vary, and experimental profiles may drastically depend on peculiarities of each particular physical system, a general probabilistic scheme resulting in the popcorn type manifestation of number-theoretic behavior in nature definitely survives.

Suppose two random integers, ϕ and ψ, are taken independently from a discrete probability distribution, $Q_n = f^n$, where $f = 1 - \varepsilon > 0$ is a damping factor. If $(p, q) = 1$, then the combination $v = \phi/(\phi + \psi)$ has the distribution given by the popcorn function in the asymptotic limit $\varepsilon \ll 1$:

$$P\left(v = \frac{p}{p+q}\right) = \sum_{n=1}^{\infty} f^{n(p+q)} = \frac{(1-\varepsilon)^{p+q}}{1-(1-\varepsilon)^{p+q}} \sim \frac{1}{\varepsilon(p+q)}\,. \quad (2)$$

The formal scheme above can be understood on the basis of the Euclid orchard construction, if one considers a directed $(1+1)$ walker on the lattice (see Fig. 1a), who performs ϕ steps along one axis of the lattice, followed by ψ steps along the other axis. At every step the walker dies with probability $\varepsilon = 1 - f$. Then, having a number of walkers starting from the origin of the lattice, one would get an 'orchard of walkers', i.e., at every spot v on the x-axis a fraction of surviving walkers $P(v)$ would be described exactly by the popcorn function.

In order to have a relevant physical picture, consider a toy model of diblock-copolymer polymerization. Without sticking to any specific polymerization mechanism, consider an ensemble of diblock-copolymers AB, polymerized independently from both ends in a cloud of monomers of the relevant kind (we assume only A–A and B–B links to be formed). Termination of polymerization is provided by specific 'radicals' of a very small concentration ε: when a radical is attached to the growing end (irrespectively, A or B), it terminates the polymerization at this extremity forever. Given the environment of infinite capacity, one assigns the probability $f = 1 - \varepsilon$ to a monomer attachment at every elementary act of the polymerization. If N_A and N_B are molecular weights of the blocks A and B, then the composition probability distribution in our ensemble, $P(\varphi = N_A/(N_A + N_B))$, in the limit of small $\varepsilon \ll 1$ is 'ultrametric' (see paper [6] for the definition of the ultrametricity) and is given by the popcorn function

$$P\left(\varphi = \frac{p}{p+q}\right) \sim \frac{1}{\varepsilon(p+q)} \stackrel{\text{def}}{=} \frac{1}{\varepsilon}\, g(\varphi)\,. \quad (3)$$

In the described process, we have assumed identical independent probabilities for the monomers of sorts ('colors') A and B to be attached at both chain ends. Since no preference is implied, one may look at this process as a homopolymer ('colorless') growth, taking place at two extremities. For this process, we are interested in statistical characteristics of the resulting ensemble of the homopolymer chains. What would play the role of 'composition' in this case, or, in other words, how should one understand the fraction of monomers attached at one end? As we show below, the answer is rather intriguing: the respective analogue of the probability distribution is the spectral density of the ensemble of linear chains with probability Q_L for the molecular mass distribution, where L is the length of a chain in the ensemble.

In our point of view, the popcorn function has not yet received proper attention among researchers, though its emergence in various physical problems seems impressive, as we demonstrate below. Apparently, the main difficulty concerns the discontinuity of $g(x)$ at every rational point, which often results in a problematic theoretical treatment and interpretation of results for the underlying physical system. Thus, a natural, physically justified 'continuous approximation' of the popcorn function is very much in demand.

Below, we provide such an approximation, showing the generality of 'popcorn-like' distributions for a class of one-dimensional disordered systems. We demonstrate that the popcorn function can be constructed on the basis of the modular Dedekind function, $\eta(x + iy)$, when the imaginary part, y, of the modular parameter $z = x + iy$ tends to 0.

2. Spectral statistics of an exponentially weighted ensemble of linear graphs

2.1 Spectral density and the popcorn function

The models explored above are intimately related to the spectral statistics of ensembles of linear polymers. In a practical setting, consider an ensemble of noninteracting linear chains with an exponential distribution of their lengths. We focus on the emergence of the fractal popcorn-like structure in the spectral density of corresponding

adjacency matrices describing the connectivity of elementary units (monomers) in linear chains.

The ensemble of exponentially weighted homogeneous chains is described by the bi-diagonal symmetric $N \times N$ adjacent matrix $B = \{b_{ij}\}$:

$$B = \begin{pmatrix} 0 & x_1 & 0 & 0 & \cdots \\ x_1 & 0 & x_2 & 0 & \\ 0 & x_2 & 0 & x_3 & \\ 0 & 0 & x_3 & 0 & \\ \vdots & & & & \ddots \end{pmatrix}, \tag{4}$$

where the distribution of each $b_{i,i+1} = b_{i+1,i} = x_i$ $(i = 1, \ldots, N)$ is Bernoullian:

$$x_i = \begin{cases} 1 & \text{with probability } f, \\ 0 & \text{with probability } \varepsilon = 1 - f. \end{cases} \tag{5}$$

We are interested in the spectral density, $\rho_\varepsilon(\lambda)$, of the ensemble of matrices B in the limit $N \to \infty$. Notice that at any $x_k = 0$, the matrix B splits into independent blocks. Every $n \times n$ block is a bi-diagonal symmetric $n \times n$ matrix A_n with all $x_k = 1$, $k = 1, \ldots, n$, which corresponds to a chain of length n. The spectrum of the matrix A_n is given by

$$\lambda_{k,n} = 2\cos\frac{\pi k}{n+1}, \qquad k = 1, \ldots, n. \tag{6}$$

All the eigenvalues $\lambda_{k,n}$ for $k = 1, \ldots, n-1$ appear with probability $Q_n = f^n$ in the spectrum of matrix (4). In the asymptotic limit $\varepsilon \ll 1$, one may deduce an equivalence between the composition distribution in the polymerization problem, discussed in the previous section, and the spectral density of the linear chain ensemble. Namely, the probability of a composition $\varphi = p/(p+q)$ in the ensemble of diblock-copolymers can be precisely mapped onto the peak intensity (the degeneracy) of the eigenvalue $\lambda = \lambda_{p,p+q-1} = 2\cos[\pi p/(p+q)]$ in the spectrum of the matrix B. In other words, the integer number k in the mode $\lambda_{k,n}$ matches the number of A-monomers, $N_\mathrm{A} = kz$, while the number of B-monomers matches $N_\mathrm{B} = (n+1-k)z$, where $z \in N$ is the respective diblock-copolymer.

The spectral statistics survive if one replaces the ensemble of Bernoullian two-diagonal adjacency matrices B defined by (4), (5) by the ensemble of random Laplacian matrices. Recall that the Laplacian matrix, $L = \{a_{ij}\}$, can be constructed from the adjacency matrix, $B = \{b_{ij}\}$, as follows: $a_{ij} = -b_{ij}$ for $i \neq j$, and $a_{ii} = \sum_{j=1}^{N} b_{ij}$. A search for eigenvalues of the Laplacian matrix L for a linear chain is equivalent to determining its relaxation spectrum. Thus, the density of the relaxation spectrum of the ensemble of noninteracting linear chains with the exponential distribution over lengths has the signature of the popcorn function.

To derive $\rho_\varepsilon(\lambda)$ for arbitrary values of ε, let us write down the spectral density of the ensemble of $N \times N$ random matrices B with the bimodal distribution of the elements as a resolvent:

$$\begin{aligned} \rho_\varepsilon(\lambda) &= \lim_{N\to\infty} \left\langle \sum_{k=1}^{n} \delta(\lambda - \lambda_{kn}) \right\rangle_{Q_n} \\ &= \lim_{\substack{N\to\infty \\ y\to+0}} y \,\mathrm{Im} \left\langle G_n(\lambda - \mathrm{i}y) \right\rangle_{Q_n} \\ &= \lim_{\substack{N\to\infty \\ y\to+0}} y \sum_{n=1}^{N} Q_n \,\mathrm{Im}\, G_n(\lambda - \mathrm{i}y), \end{aligned} \tag{7}$$

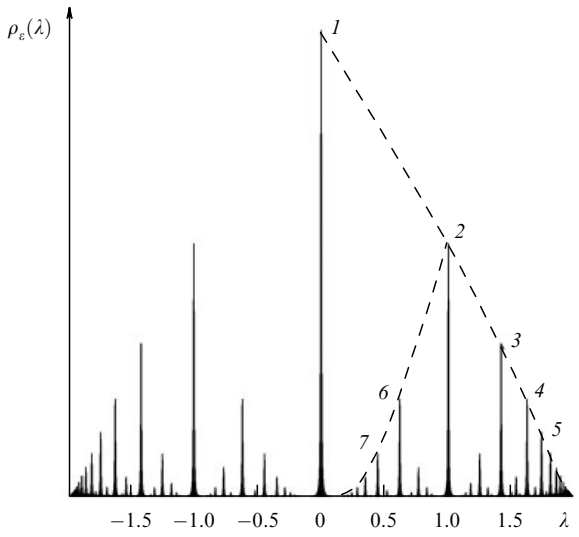

Figure 2. Spectral density $\rho_\varepsilon(\lambda)$ for an ensemble of bi-diagonal matrices of size $N = 10^3$ at $f = 0.7$. The regularization parameter ε is taken equal to 2×10^{-3}.

where $\langle \ldots \rangle_{Q_n}$ means averaging over the distribution $Q_n = (1-\varepsilon)^n$, and the following regularization of the Kronecker δ-function is used:

$$\delta(\xi) = \lim_{y\to+0} \mathrm{Im}\, \frac{y}{\xi - \mathrm{i}y}. \tag{8}$$

The function G_n is associated with each particular gapless matrix B of n sequential '1' on the subdiagonals:

$$G_n(\lambda - \mathrm{i}y) = \sum_{k=1}^{n} \frac{1}{\lambda - \lambda_{k,n} - \mathrm{i}y}. \tag{9}$$

Collecting formulas (6), (7), and (9), we find an explicit expression for the density of eigenvalues:

$$\rho_\varepsilon(\lambda) = \lim_{\substack{N\to\infty \\ y\to+0}} y \sum_{n=1}^{N} (1-\varepsilon)^n \sum_{k=1}^{n} \frac{y}{\left\{\lambda - 2\cos\left[\pi k/(n+1)\right]\right\}^2 + y^2}. \tag{10}$$

The behavior of the inner sum in the spectral density in the asymptotic limit $y \to 0$ is easy to understand: it is $1/y$ at $\lambda = 2\cos[\pi k/(n+1)]$, and zero otherwise. Thus, one can already infer a qualitative similarity with the popcorn function. It turns out that the correspondence is quantitative for $\varepsilon = 1 - f \ll 1$. Driven by the purpose to show it, we calculate the values of $\rho_\varepsilon(\lambda)$ at the peaks, i.e., at rational points $\lambda = 2\cos[\pi p/(p+q)]$ with $(p,q) = 1$ and end up with a similar geometrical progression as for the case of diblock-copolymer problem (2):

$$\begin{aligned} \rho_\varepsilon\left(\lambda = 2\cos\frac{\pi p}{p+q}\right) &= \sum_{s=1}^{\infty} (1-\varepsilon)^{(p+q)s-1} \\ &= \frac{(1-\varepsilon)^{p+q-1}}{1-(1-\varepsilon)^{p+q}}\bigg|_{\varepsilon\to0} \sim \frac{1}{\varepsilon(p+q)} \stackrel{\mathrm{def}}{=} g\left(\frac{1}{\pi}\arccos\frac{\lambda}{2}\right). \end{aligned} \tag{11}$$

The typical sample plot $\rho_\varepsilon(\lambda)$ for $f = 0.7$ computed numerically via expression (10) with $\varepsilon = 2 \times 10^{-3}$ is shown in Fig. 2 for $N = 10^3$.

2.2 Enveloping curves and tails of the eigenvalues density

Below, we focus on some number-theoretic properties of the spectral density of the argument λ, since in this case the correspondence with the composition ratio is precise. One can compute the enveloping curves for any monotonic sequence of peaks depicted in Fig. 2, where we show two series of sequential peaks: $S_1 = \{1-2-3-4-5-\ldots\}$ and $S_2 = \{2-6-7-\ldots\}$. Any monotonic sequence of peaks corresponds to the set of eigenvalues $\lambda_{k,n}$ constructed on the basis of a Farey sequence [7]. For example, as shown below, the peaks in the series S_1 are located at

$$\lambda_k = -\lambda_{k,k} = -2\cos\frac{\pi k}{k+1}\,, \qquad k = 1, 2, \ldots,$$

while the peaks in the series S_2 are located at

$$\lambda_{k'} = -\lambda_{k',\,2k'-2} = -2\cos\frac{\pi k'}{2k'-1}\,, \qquad k' = 2, 3, \ldots\,.$$

The positions of the peaks obey the following rule: let $\{\lambda_{k-1},\, \lambda_k,\, \lambda_{k+1}\}$ be three consecutive monotonically ordered peaks (e.g., peaks $2-3-4$ in Fig. 2), and let

$$\lambda_{k-1} = -2\cos\frac{\pi p_{k-1}}{q_{k-1}}\,, \quad \lambda_{k+1} = -2\cos\frac{\pi p_{k+1}}{q_{k+1}}\,,$$

where p_k and q_k $(k = 1, \ldots, N)$ are coprimes. The position of the intermediate peak, λ_k, is defined as

$$\lambda_k = -2\cos\frac{\pi p_k}{q_k}\,, \qquad \frac{p_k}{q_k} = \frac{p_{k-1}}{q_{k-1}} \oplus \frac{p_{k+1}}{q_{k+1}} \equiv \frac{p_{k-1}+p_{k+1}}{q_{k-1}+q_{k+1}}\,. \quad (12)$$

The sequences of coprime fractions constructed via the $\oplus$ addition are known as Farey sequences. A simple geometric model behind the Farey sequence, known as Ford circles [8], is shown in Fig. 3a. In brief, the construction goes as follows.

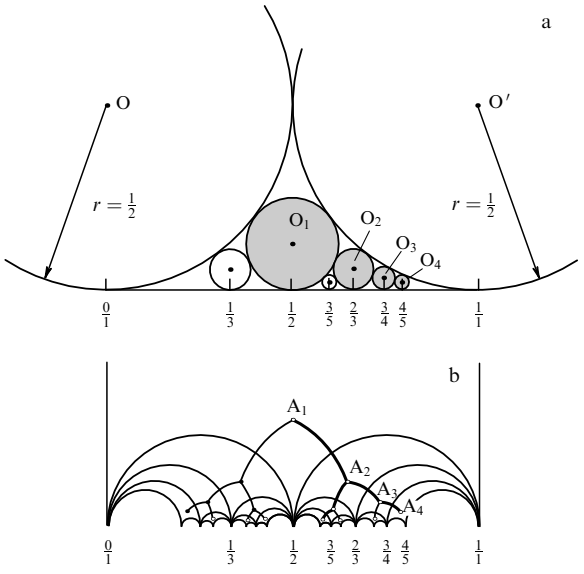

Figure 3. Ford circles as an illustration of the Farey sequence construction. (a) Each circle touches two neighbors (right and left) and the segment. The position of the newly generated circle is determined via the $\oplus$ addition: $p_{k-1}/q_{k-1} \oplus p_{k+1}/q_{k+1} = (p_{k-1}+p_{k+1})/(q_{k-1}+q_{k+1})$. (b) The same Farey sequence generated by sequential fractional-linear transformations of the fundamental domain of the modular group $\mathrm{SL}(2, Z)$.

Take the segment $[0, 1]$ and draw two circles O and O′, both of radius $r = 1/2$, which touch each other and the segment at the points 0 and 1. Now inscribe a new circle O_1 touching O, O′ and $[0, 1]$. Where is the position of the new circle along the segment? The generic recursive algorithm constitutes the Farey sequence construction. Notice that the same Farey sequence can be sequentially generated by fractional-linear transformations (reflections with respect to the arcs) of the fundamental domain of the modular group $\mathrm{SL}(2, Z)$ — the triangle lying in the upper half-plane $\mathrm{Im}\, z > 0$ of the complex plane z (see Fig. 3b).

Consider the main peak sequence

$$S_1 = \{1-2-3-4-5-\ldots\}\,.$$

The explicit expression for their positions reads

$$\lambda_k = -2\cos\frac{\pi k}{k+1}\,, \qquad k = 1, 2, \ldots\,. \quad (13)$$

One can straightforwardly investigate the asymptotic behavior of the popcorn function in the limit of $k \to \infty$. From progression (11), for arbitrary $f < 1$ we have the set of parametric equations

$$\begin{cases} \rho_\varepsilon(\lambda_k) = \dfrac{f^k}{1-f^{k+1}}\Big|_{k\gg 1} \sim f^k\,, \\ \lambda_k = -2\cos\dfrac{\pi k}{k+1}\Big|_{k\gg 1} \sim 2 - \dfrac{\pi^2}{k^2}\,. \end{cases} \quad (14)$$

From the second equation of Eqn (14), we get $k \sim \pi/\sqrt{2-\lambda}$. Substituting this expression into the first one of Eqn (14), we end up with the following asymptotic behavior of the spectral density near the spectral edge $\lambda \to 2^-$:

$$\rho_\varepsilon(\lambda) \sim \exp\left(-\frac{\pi|\log f|}{\sqrt{2-\lambda}}\right), \qquad 0 < f < 1\,. \quad (15)$$

Behavior of Eqn (14) is the signature of the Lifshitz tail typical of the 1D Anderson localization:

$$\rho_\varepsilon(E) \sim \exp\left(-CE^{-D/2}\right), \quad (16)$$

where $E = 2 - \lambda$ and $D = 1$.

3. From the popcorn function to the Dedekind η-function

3.1 Some facts about the Dedekind η-function and its related series

The popcorn function has discontinuous maxima at rational points and continuous valleys at irrationals. We show in this section that the popcorn function can be regularized on the basis of the everywhere continuous Dedekind function $\eta(x + \mathrm{i}y)$ in the asymptotic limit $y \to 0$.

The famous Dedekind η-function is defined as follows:

$$\eta(z) = \exp\left(\frac{\pi \mathrm{i} z}{12}\right)\prod_{n=0}^{\infty}\left[1 - \exp\left(2\pi \mathrm{i} n z\right)\right]. \quad (17)$$

The argument $z = x + \mathrm{i}y$ is called the modular parameter, and $\eta(z)$ is defined for $\mathrm{Im}\, z > 0$ only. The Dedekind

η-function is invariant with respect to the action of the modular group $\mathrm{SL}(2,\mathbb{Z})$:

$$\eta(z+1) = \exp\left(\frac{\pi \mathrm{i} z}{12}\right)\eta(z)\,, \qquad \eta\left(-\frac{1}{z}\right) = \sqrt{-\mathrm{i}}\,\eta(z)\,. \tag{18}$$

And, in general, one has

$$\eta\left(\frac{az+b}{cz+d}\right) = \omega(a,b,c,d)\,\sqrt{cz+d}\,\eta(z)\,, \tag{19}$$

where $ad-bc=1$, and $\omega(a,b,c,d)$ is some root of the 24th degree of unity [10].

It is convenient to introduce the following 'normalized' function

$$h(z) = \left|\eta(z)\right|(\mathrm{Im}\, z)^{1/4}\,. \tag{20}$$

The real analytic Eisenstein series $E(z,s)$ is defined in the upper half-plane, $H=\{z\colon \mathrm{Im}\, z>0\}$ for $\mathrm{Re}\, s>1$ as follows:

$$E(z,s) = \frac{1}{2}\sum_{\{m,n\}\in\mathbb{Z}^2\setminus\{0,0\}}\frac{y^s}{|mz+n|^{2s}}\,, \qquad z=x+\mathrm{i}y\,. \tag{21}$$

This function can be analytically continued to the entire s plane with one simple pole at $s=1$. Notably, it shares the same invariance properties in z as the Dedekind η-function. Moreover, $E(s,z)$, as a function of z, is the $\mathrm{SL}(2,\mathbb{Z})$-automorphic solution of the hyperbolic Laplace equation

$$-y^2\left(\frac{\partial^2}{\partial x^2}+\frac{\partial^2}{\partial y^2}\right)E(z,s) = s(1-s)\,E(z,s)\,.$$

The Eisenstein series is closely related to the Epstein ζ-function, $\zeta(s,Q)$, namely

$$\zeta(s,Q) = \sum_{\{m,n\}\in\mathbb{Z}^2\setminus\{0,0\}}\frac{1}{Q(m,n)^s} = \frac{2}{d^{s/2}}\,E(z,s)\,, \tag{22}$$

where $Q(m,n)=am^2+2bmn+cn^2$ is a positive definite quadratic form, $d=ac-b^2>0$, and $z=(-b+\mathrm{i}\sqrt{d})/a$. Eventually, the logarithm of the Dedekind η-function is known to enter into the Laurent expansion of the Epstein ζ-function. Its residue at $s=1$ has been calculated by Dirichlet and is known as the first Kronecker limit formula [11–13]. Explicitly, as $s\to 1$ it reads

$$\zeta(s,Q) = \frac{\pi}{\sqrt{d}}\frac{1}{s-1}+\frac{2\pi}{\sqrt{d}}\left(\gamma+\ln\sqrt{\frac{a}{4d}}-2\ln\left|\eta(z)\right|\right) + O(s-1)\,. \tag{23}$$

Equation (23) establishes the important connection between the Dedekind η-function and the respective series, which we substantially exploit below.

3.2 Relation between the popcorn function and Dedekind η-function

Consider an arbitrary quadratic form $Q'_x(m,n)$ with a unit determinant. Since $d=1$, it can be written in new parameters $\{a,b,c\}\to\{x=b/c,\varepsilon=1/c\}$ as follows:

$$Q'_x(m,n) = \frac{1}{\varepsilon}(xm-n)^2+\varepsilon m^2\,. \tag{24}$$

Applying the first Kronecker limit formula to the Epstein function with quadratic form (24) and $s=1+\tau$, where $\tau\ll 1$, but finite, we get

$$\zeta(s,Q'_x) = \frac{\pi}{s-1}+2\pi\left(\gamma+\ln\sqrt{\frac{1}{4\varepsilon}}-2\ln\left|\eta(x+\mathrm{i}\varepsilon)\right|\right) + O(s-1)\,. \tag{25}$$

On the other hand, use can be made of the ε-continuation of the Kronecker δ-function (8), and $\zeta(1+\tau,Q'_x)$ for small $\tau\ll 1$ can be assessed as follows:

$$\zeta(1+\tau,Q'_x) \sim \frac{1}{\varepsilon}\sum_{\{m,n\}\in\mathbb{Z}^2\setminus\{0,0\}}\frac{\varepsilon^2}{(xm-n)^2+\varepsilon^2 m^2} = \frac{2}{\varepsilon}\lim_{N\to\infty}\sum_{m=1}^{N}\sum_{n=1}^{N}\frac{1}{m^2}\,\delta\left(x-\frac{n}{m}\right)\equiv\theta(x)\,, \tag{26}$$

where $x\in(0,1)$, and the factor 2 reflects the presence of two quadrants on the $\mathbb{Z}^2$-lattice that contribute jointly to the sum at every rational point, while θ assigns 0 to all irrationals. At rational points, $\theta(p/q)$ can be calculated straightforwardly:

$$\theta\left(\frac{p}{q}\right) = \frac{2}{\varepsilon}\sum_{m\,\vdots\,q}^{\infty}\frac{1}{m^2} = \frac{\pi^2}{3\varepsilon q^2}\,, \tag{27}$$

where the symbol $\vdots$ denotes the division in whole numbers. Comparing formula (27) with the definition of the popcorn function, g, one ends up with the following relation at the peaks:

$$g\left(\frac{p}{q}\right) = \sqrt{\frac{3\varepsilon}{\pi^2}\,\theta\left(\frac{p}{q}\right)}\,. \tag{28}$$

Eventually, collecting Eqns (25) and (28), we may write down the regularization of the popcorn function by the Dedekind $\eta(x+\mathrm{i}\varepsilon)|_{\varepsilon\to 0}$ function in the interval $0<x<1$:

$$g(x) \sim \left.\sqrt{-\frac{12\varepsilon}{\pi}\ln\left|\eta(x+\mathrm{i}\varepsilon)\right|-o(\varepsilon\ln\varepsilon)}\right|_{\varepsilon\to 0}\,, \tag{29}$$

or

$$-\ln\left|\eta(x+\mathrm{i}\varepsilon)\right|_{\varepsilon\to 0} \sim \frac{\pi}{12\varepsilon}\,g^2(x)\,. \tag{30}$$

Notice that the asymptotic behavior of the Dedekind η-function can be independently derived through duality relations [6]. However, such an approach leaves in the dark the underlying structural equivalence of the popcorn and η functions and their series representation on the lattice $\mathbb{Z}^2$. In Fig. 4, we show two discrete plots of the left- and right-hand sides of formula (30).

Thus, the spectral density of the ensemble of linear chains, (11), in the regime $\varepsilon\ll 1$ is expressed through the Dedekind η-function as follows:

$$\rho_\varepsilon(\lambda) \sim \sqrt{-\frac{12}{\pi\varepsilon}\ln\left|\eta\left(\frac{1}{\pi}\arccos\frac{\lambda}{2}+\mathrm{i}\varepsilon\right)\right|}\,. \tag{31}$$

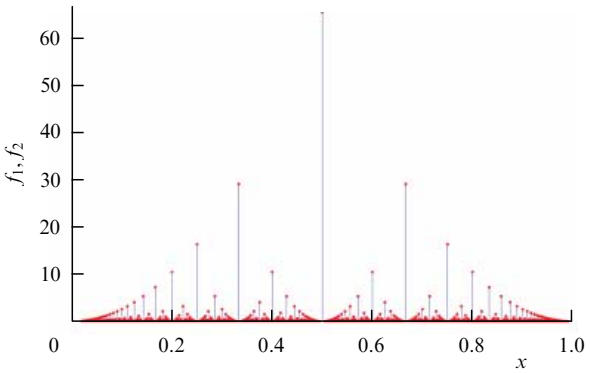

Figure 4. (Color online.) Plots of everywhere continuous function $f_1(x) = -\ln|\eta(x+i\varepsilon)|$ (blue) and discrete function $f_2(x) = (\pi/12\varepsilon)g^2(x)$ (red) for $\varepsilon = 10^{-6}$ at rational points in $0 < x < 1$.

4. Conclusion

We have discussed the number-theoretic properties of distributions appearing in physical systems, when an observable is a quotient of two independent exponentially weighted integers. The spectral density of the ensemble of linear polymer chains distributed with the law f^L $(0 < f < 1)$, where L is the chain length, serves as a particular example. As $f \to 1$, the spectral density can be expressed through the Thomae ('popcorn') function, discontinuous and nondifferentiable at all rational points. We suggest a continuous approximation of the popcorn function, based on the Dedekind η-function near the real axis.

Analysis of the spectrum at the edges reveals Lifshitz tails, typical of 1D Anderson localization. The nontrivial feature, related to the asymptotic behavior of the shape of the spectral density of the adjacency matrix, is as follows. The main, enveloping, sequence of peaks $1-2-3-4-5-\ldots$ in Fig. 2 has the asymptotic behavior $\rho(\lambda) \sim q^{\pi/\sqrt{2-\lambda}}$ (as $\lambda \to 2^-$) typical of 1D Anderson localization; however, any internal subsequence of peaks, like $2-6-7-\ldots$, has the asymptotic behavior $\rho'(\lambda) \sim q^{\pi/|\lambda-\lambda_{\rm cr}|}$ (as $\lambda \to \lambda_{\rm cr}$), which is reminiscent of the Anderson localization in 2D.

We would like to emphasize that the ultrametric structure of the spectral density is ultimately related to number-theoretic properties of modular functions. We also pay attention to the connection between the popcorn function and the invariant measures of some continued fractions studied by Borwein and Borwein in 1993 [17].

The notion of ultrametricity deals with the concept of a hierarchical organization of energy landscapes [19, 20]. A complex system is assumed to have a large number of metastable states corresponding to local minima in the potential energy landscape. With respect to the transition rates, the minima are suggested to be clustered in hierarchically nested basins, i.e., larger basins consist of smaller basins, each of these consists of even smaller ones, etc. The basins of local energy minima are separated by a hierarchically arranged set of barriers: large basins are separated by high barriers, and smaller basins within each larger one are separated by lower barriers. Ultrametric geometry fixes taxonomic (i.e., hierarchical) tree-like relationships between elements and, speaking figuratively, is closer to the Lobachevsky geometry than to the Euclidean one [21, 22].

Acknowledgments

We are very grateful to V Avetisov, A Gorsky, Yu Fedorov, and P Krapivsky for many illuminating discussions. This study was partially supported by IRSES (International Research Staff Exchange Scheme), DIONICOS (Dynamic of and in Complex Systems) and RFBR 16-02-00252a grants.

References

1. Beanland K, Roberts J W, Stevenson C *Am. Math. Monthly* **116** 531 (2009)
2. Trifonov V et al. *Sci. Rep.* **1** 191 (2011)
3. Planat M, Eckert C *IEEE Trans. Ultrasonics Ferroelectrics Frequency Control* **47** 1173 (2000)
4. Lundholm D *Phys. Rev. A* **96** 012116 (2017); arXiv:1608.05067
5. Middendorf M, Ziv E, Wiggins C H *Proc. Natl. Acad. Sci. USA* **102** 3192 (2005)
6. Avetisov V, Krapivsky P L, Nechaev S *J. Phys. A* **49** 035101 (2016)
7. Hardy G H, Wright E M *An Introduction to the Theory of Numbers* (New York: Oxford Univ. Press, 1979)
8. Ford L R *Am. Math. Monthly* **45** 586 (1938)
9. Coxeter H S M *Am. Math. Monthly* **75** 5 (1968)
10. Chandrasekharan K *Elliptic Functions* (Berlin: Springer-Verlag, 1985)
11. Epstein P *Math. Ann.* **56** 615 (1903)
12. Siegel C L *Lectures on Advanced Analytic Number Theory* (Mumbai: Tata Institute of Fundamental Research, 1961)
13. Motohashi Y *Proc. Jpn. Acad.* **44** 614 (1968)
14. Dyson F J *Phys. Rev.* **92** 1331 (1953)
15. Domb C et al. *Phys. Rev.* **115** 18 (1959)
16. Nieuwenhuizen Th M, Luck J M *J. Stat. Phys.* **41** 745 (1985)
17. Borwein J M, Borwein P B *J. Number Theory* **43** 293 (1993)
18. Comtet A, Nechaev S *J. Phys. A* **31** 5609 (1998)
19. Mezard M, Parisi G, Virasoro M A *Spin Glass Theory and Beyond* (World Scientific Lecture Notes in Physics, Vol. 9) (Singapore: World Scientific, 1987)
20. Frauenfelder H, in *Protein Structure: Molecular and Electronic Reactivity. Proc. of a Conf., April 10–13, 1985, Philadelphia, Pa., USA* (Eds R Austin et al.) (New York: Springer-Verlag, 1987) p. 245
21. Nechaev S, Polovnikov K *Soft Matter* **13** 1420 (2017)
22. Levitov L S *Europhys. Lett.* **14** 533 (1991)